

# Detection of Texture Objects on Multichannel Images

Elena Medvedeva, Alena Evdokimova  
 Vyatka State University, VyatSU  
 Kirov, Russia  
 emedv@mail.ru, alenaevdokimova0@gmail.com

**Abstract**—A method for detecting extended texture objects on multi-channel images is proposed. The method is based on the representation of multi-digit digital images by a set of bit images and their approximation by three-dimensional Markov chains with two states. It is proposed to use transition probabilities for three-dimensional Markov chains and brightness characteristics averaged within a sliding window as textural features. To reduce computational resources, determination of signs is carried out by the bit planes of the senior, most informative digits of the digital image. The detection of texture objects is based on the analysis of the histogram of the texture feature and the brightness of the pixels. The simulation results confirm the effectiveness of the proposed method.

## I. INTRODUCTION

A number of modern video systems tend to use multi-channel images, an example of which can be multispectral images. Multispectral remote sensing images have high spatial resolution and contain a lot of information about the texture. Information about the texture allows to determine the types of the earth's surface (rocks, soil, vegetation, water, etc.), to estimate the areas of flooding, land use, forestry, wildfires, oil pollution, ice, etc. The ability to detect textural objects in multispectral images is based on the fact that objects of different types reflect and absorb electromagnetic radiation in different wavelengths in different ways. When combining different channels, one can find out information about rocks, vegetation cover, state of reservoirs, types of agricultural crops, etc. For example, in the visible red spectral channel (wavelength 0.63–0.69  $\mu\text{m}$ ), many plant varieties can be distinguished [1], [2]. And the visible blue channel (wavelength 0.45–0.52  $\mu\text{m}$ ) is intended to display coasts, sediments; soil differentiation from vegetation, mapping forest types, detection of artificial structures [1], [2].

The basic operation for detecting edges of texture objects is segmentation, the quality of which is determined by the effectiveness of the selection of a textural feature. There are various approaches to the selection of textures [1], [3]–[12], the most important of which are: statistical, spectral and structural. Structural methods are effective in the analysis of regular textures, spectral - when searching the image. More universal are statistical methods in which adjacency matrices, autocorrelation, differences in gray levels, the local frequency of brightness fluctuations, etc. are used as statistical characteristics.

Assuming that the texture regions on the images occupy extended regions with homogeneous statistical characteristics and different for different regions, therefore, a statistical approach based on the mathematical apparatus of Markov chains [9], [13] is very effective, the complexity of which depends on the dimension of transition probability matrices.

Works [14], [15] propose to solve the computational complexity reduction problem using representation of  $g$  - bit digital images (DI) as a set of  $g$  - bit binary images (BBI) and approximate them with Markov chains with two states and  $2 \times 2$  transition probability matrices. Assuming that the most informative are the binary images belonging to the senior bits of DI, it is proposed to use one of the BBIs of the senior bits of DI to select textures. This solution reduces computational resources in the allocation of textures.

When using the mathematical apparatus of Markov chains, textural features are probabilistic characteristics between elements of images. Works [16]–[18] present the method of texture segmentation of DI based on a two-dimensional Markov chain with two states. With probabilities of transitions between elements different by 0.15 for different texture areas, the segmentation error did not exceed 6%.

Considering that there is a large statistical dependence between separate areas of images taken in different spectral ranges (channels), it is proposed to use the nature of the statistical connection not only between the elements inside the DI, but also the inter-channel DI. The use of the transition probability for three-dimensional Markov chains as a textural attribute improves the accuracy of prediction of image elements and, accordingly, the quality of the selection of textures. Also, an approach based on three-dimensional Markov chains can be applied to detect changed texture regions in time-varying DIs.

Real remote sensing DIs contain objects in which the pixel brightness changes slightly (water bodies, fields of different crops, etc.). Therefore, to improve the quality of detection of texture objects for which the probabilistic characteristics between the elements are close to unity, it is advisable to take into account the brightness characteristics determined by BBI of the senior bits DI.

The aim of the article is to develop a method of segmentation of multi-channel digital images with high spatial resolution based on the mathematical apparatus of three-dimensional Markov chains, which allows to increase the

accuracy of detecting the edges of texture objects while reducing computational resources.

This paper is structured as follows. Section II describes the three-dimensional segmentation method based on a mathematical model of three-dimensional Markov chain images. Section III presents experimental results and comparisons. Section IV presents conclusions.

## II. TEXTURE-BASED THREE-DIMENSIONAL SEGMENTATION METHOD

### A. Mathematical model of multichannel image

A special case of multichannel images can be considered color RGB images. Therefore, the proposed method will be considered for the case of three-component DI with R, G, and B color channels. Each RGB color component of an image is a g-digit digital half tone image. There is a significant statistical relationship between the elements of individual DI areas belonging to different color channels. For example, objects of yellow color are well expressed on green and red components, and objects of white color are seen on all three components. Therefore, taking into account the statistical connection between the elements inside DI and between individual color channels, we can assume that RGB images allow them to be approximated by a three-dimensional Markov chain with several states, and BBI with a three-dimensional Markov chain with two states and horizontal transition matrices

$${}^1\Pi^{(l)} = \begin{Bmatrix} 1 & 1 \\ \pi_{11}^{(l)} & \pi_{12}^{(l)} \\ \pi_{21}^{(l)} & \pi_{22}^{(l)} \end{Bmatrix}, \text{ vertical } {}^2\Pi^{(l)} = \begin{Bmatrix} 2 & 2 \\ \pi_{11}^{(l)} & \pi_{12}^{(l)} \\ \pi_{21}^{(l)} & \pi_{22}^{(l)} \end{Bmatrix} \text{ and}$$

$${}^4\Pi^{(l)} = \begin{Bmatrix} 4 & 4 \\ \pi_{11}^{(l)} & \pi_{12}^{(l)} \\ \pi_{21}^{(l)} & \pi_{22}^{(l)} \end{Bmatrix}, (l = \overline{1, g}) \text{ between channels. The}$$

introduction of the inter-channel matrix  ${}^4\Pi^{(l)}$  will make it possible to get rid of the segmentation of the separate components and identify the changed areas in the images.

Fig. 1 shows a fragment of an BBI with two color components.

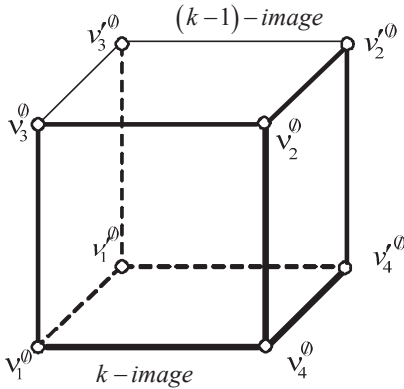


Fig. 1. Fragment of BBI of two color components

The amount of information in the element  $v_4^{(l)}$  relative to the elements of the nearest neighborhood  $\Lambda_{i,j,k} = \{v_1^{(l)}, v_2^{(l)}, v_4^{(l)}\}$ , in accordance with the mathematical model of the three-dimensional random Markov process presented in [14], [15], is determined by the formula:

$$I(v_4^{(l)} | v_1^{(l)}, v_2^{(l)}, v_4^{(l)}) = I(v_4^{(l)}) - I(v_1^{(l)}, v_2^{(l)}, v_4^{(l)}, v_4^{(l)}) =$$

$$= -\left[ \log p(v_4^{(l)}) + \log \frac{\prod_{i=1}^4 p(v_i^{(l)}, v_j^{(l)}) p(v_1^{(l)}, v_2^{(l)}, v_4^{(l)}, v_4^{(l)})}{\prod_{i=1}^4 p(v_i^{(l)}) \prod p(v_i^{(l)}, v_j^{(l)}, v_k^{(l)})} \right] =$$

$$= -\log \frac{\prod_{i=1}^3 w(v_4^{(l)} | v_i^{(l)}) w(v_4^{(l)} | v_1^{(l)}, v_2^{(l)}, v_4^{(l)})}{\prod w(v_4^{(l)} | v_i^{(l)}, v_j^{(l)})}, \quad (1)$$

where  $p(v_i^{(l)})$  is the a priori probability density of element values;  $p(v_i^{(l)}, v_j^{(l)})$ ,  $p(v_i^{(l)}, v_j^{(l)}, v_k^{(l)})$ ,  $p(v_1^{(l)}, v_2^{(l)}, v_4^{(l)}, v_4^{(l)})$ ,  $i = j = k = \overline{1, 4}$ ;  $i \neq j \neq k$  are joint probability density values of the elements;  $w(v_4^{(l)} | v_i^{(l)})$ ,  $i = \overline{1, 3}$ ; are one-dimensional density of probabilities of transitions;  $w(v_4^{(l)} | v_i^{(l)}, v_j^{(l)})$ ,  $i = j = \overline{1, 3}$ ;  $i \neq j$  are probability density of transitions in two-dimensional Markov chains;  $w(v_4^{(l)} | v_1^{(l)}, v_2^{(l)}, v_4^{(l)})$  are probability density of transitions in three-dimensional Markov chains.

The probability density of transitions in a three-dimensional binary Markov chain  $w(v_4^{(l)} | \Lambda_{i,j,k}^{(l)})$  can have the form:

$$w(v_4^{(l)} | \Lambda_{i,j,k}^{(l)}) =$$

$$= \sum_{i, \dots, r=1}^2 \pi(v_4^{(l)} = M_i^{(l)} | v_1^{(l)} = M_j^{(l)};$$

$$v_2^{(l)} = M_k^{(l)}, v_4^{(l)} = M_r^{(l)}) \times$$

$$\delta(v_1^{(l)} - M_j^{(l)}) \delta(v_2^{(l)} - M_k^{(l)}) \delta(v_4^{(l)} - M_r^{(l)}). \quad (2)$$

where  $\delta(\cdot)$  is the delta function.

Taking into account the (1) transition probability matrix  $\Pi$  for various combinations elements states of the neighborhood  $\Lambda_{i,j,k}^{(l)}$  has the form:

$$\Pi = \begin{pmatrix} \pi_{iii}^{(l)} & \pi_{iij}^{(l)} \\ \pi_{iji}^{(l)} & \pi_{ijj}^{(l)} \\ \pi_{jii}^{(l)} & \pi_{jjj}^{(l)} \\ \pi_{jji}^{(l)} & \pi_{jij}^{(l)} \\ \pi_{jij}^{(l)} & \pi_{jji}^{(l)} \\ \pi_{jji}^{(l)} & \pi_{jij}^{(l)} \\ \pi_{jij}^{(l)} & \pi_{jji}^{(l)} \\ \pi_{jji}^{(l)} & \pi_{jij}^{(l)} \end{pmatrix} = \begin{pmatrix} \alpha_1^{(l)} & \alpha_1'^{(l)} \\ \alpha_2^{(l)} & \alpha_2'^{(l)} \\ \alpha_3^{(l)} & \alpha_3'^{(l)} \\ \alpha_4^{(l)} & \alpha_4'^{(l)} \\ \alpha_5^{(l)} & \alpha_5'^{(l)} \\ \alpha_6^{(l)} & \alpha_6'^{(l)} \\ \alpha_7^{(l)} & \alpha_7'^{(l)} \\ \alpha_8^{(l)} & \alpha_8'^{(l)} \end{pmatrix}, i, j = \overline{1, 2}; i \neq j, \quad (3)$$

elements of which satisfy the normalization requirement  $\alpha_q^{(l)} + \alpha_q'^{(l)} = 1$ .

The probabilities of the states  $\pi_{iii}^{(l)}$  of an element  $v_4^{(l)}$  are determined by the argument of expression (1) and for various combinations of neighboring elements  $\Lambda_{i,j,k}^{(l)}$  can be calculated using the formulae presented in Table I.

TABLE I. EXPRESSIONS FOR CALCULATING CONDITIONAL PROBABILITIES.

$v_1 v_2 v_3 \rightarrow v_4$	Выражения
000 → 0	$\pi_{iii}^{(l)} = \frac{1 \pi_{ii}^{(l)} \cdot 2 \pi_{ii}^{(l)} \cdot 4 \pi_{ii}^{(l)} \cdot 7 \pi_{ii}^{(l)}}{3 \pi_{ii}^{(l)} \cdot 5 \pi_{ii}^{(l)} \cdot 6 \pi_{ii}^{(l)}}$ ,
001 → 0	$\pi_{iij}^{(l)} = \frac{1 \pi_{ii}^{(l)} \cdot 2 \pi_{ii}^{(l)} \cdot 4 \pi_{ij}^{(l)} \cdot 7 \pi_{ij}^{(l)}}{3 \pi_{ii}^{(l)} \cdot 5 \pi_{ij}^{(l)} \cdot 6 \pi_{ij}^{(l)}}$ ,
⋮	⋮
111 → 0	$\pi_{jii}^{(l)} = \frac{1 \pi_{ij}^{(l)} \cdot 2 \pi_{ij}^{(l)} \cdot 4 \pi_{ij}^{(l)} \cdot 7 \pi_{ij}^{(l)}}{3 \pi_{ii}^{(l)} \cdot 5 \pi_{ii}^{(l)} \cdot 6 \pi_{ii}^{(l)}}$ ,
000 → 1	$\pi_{iij}^{(l)} = \frac{1 \pi_{ij}^{(l)} \cdot 2 \pi_{ij}^{(l)} \cdot 4 \pi_{ij}^{(l)} \cdot 7 \pi_{ij}^{(l)}}{3 \pi_{ii}^{(l)} \cdot 5 \pi_{ii}^{(l)} \cdot 6 \pi_{ii}^{(l)}}$ ,
001 → 1	$\pi_{ijj}^{(l)} = \frac{1 \pi_{ij}^{(l)} \cdot 2 \pi_{ij}^{(l)} \cdot 4 \pi_{ii}^{(l)} \cdot 7 \pi_{ii}^{(l)}}{3 \pi_{ii}^{(l)} \cdot 5 \pi_{ij}^{(l)} \cdot 6 \pi_{ij}^{(l)}}$ ,
⋮	⋮
111 → 1	$\pi_{jij}^{(l)} = \frac{1 \pi_{ii}^{(l)} \cdot 2 \pi_{ii}^{(l)} \cdot 4 \pi_{ii}^{(l)} \cdot 7 \pi_{ii}^{(l)}}{3 \pi_{ii}^{(l)} \cdot 5 \pi_{ii}^{(l)} \cdot 6 \pi_{ii}^{(l)}}$ ,

where  ${}^r \pi_{ii}^{(l)} (r = \overline{1, 7})$  are elements of transition probability matrices in one-dimensional Markov chains with two states of three main -  ${}^1 \Pi^{(l)}$ ,  ${}^2 \Pi^{(l)}$ ,  ${}^4 \Pi^{(l)}$  and four related matrices –

$$\begin{aligned} {}^3 \Pi^{(l)} &= {}^1 \Pi^{(l)} \times {}^2 \Pi^{(l)}, {}^5 \Pi^{(l)} = {}^1 \Pi^{(l)} \cdot {}^4 \Pi^{(l)}, \\ {}^6 \Pi^{(l)} &= {}^2 \Pi^{(l)} \cdot {}^4 \Pi^{(l)}, {}^7 \Pi^{(l)} = {}^3 \Pi^{(l)} \cdot {}^4 \Pi^{(l)}. \end{aligned}$$

*B. Texture 3D Segmentation Algorithm*

Allocation of extended textures in multichannel (or multi-temporal) DI was reduced to calculating estimates of transition probabilities horizontally  ${}^1 \hat{\pi}_{ii}^{(l)}$ , vertically  ${}^2 \hat{\pi}_{ii}^{(l)}$ , between channels  ${}^4 \hat{\pi}_{ii}^{(l)}$  and estimation  $\hat{\pi}_{iii}^{(l)}$  using formulas (4), as well as estimating brightness in BBI of the senior, most informative DI digits.

Taking into account the local changes in the probability and brightness characteristics on multichannel images, a three-dimensional sliding window was used for calculation. The size of the window is determined based on predetermined estimation accuracy and minimal computational cost.

It was shown in [16]-[18] that small windows lead to a significant heterogeneity of the segmented regions, but in this case it is possible to exactly localize regions borders. Large windows ensure homogeneity of segmented regions; however, it is not possible to exactly localize regions borders. Windows from 11×11 to 21× 21 elements are acceptable for most textures and are most effective from the viewpoint of the segmentation quality/processing time ratio [16].

The texture features were the average estimates corresponding to the central element of the window -  $\hat{\pi}_{iii}^{(l,r,k)}$  of probability of transitions in the three-dimensional Markov chain and the brightness  $\tilde{L}^{(l,r,k)}$  of the BBI:

$$\hat{\pi}_{iii}^{(l,r,k)} = \frac{1}{m \times n} \sum_{r=1}^m \sum_{k=1}^n \hat{\pi}_{iii}^{(l,r,k)}. \quad (5)$$

$$\tilde{L}^{(l,r,k)} = \frac{1}{m \times n} \sum_{r=1}^m \sum_{k=1}^n \tilde{L}^{(l,r,k)}. \quad (6)$$

The pixel belonging to one or another texture object in the image of the k- channel was carried out on the basis of the analysis of the texture feature histogram [19]. The number of peaks in the histogram corresponded to the number of texture objects with different probabilistic characteristics. The threshold value was chosen as the minimum value between two adjacent peaks of the histogram. When evaluation  $\hat{\pi}_{iii}^{(l,r,k)}$  was close to 1, the averaged brightness  $\tilde{L}$  was additionally used to decide whether a pixel belongs to one or another object. Each texture object was assigned its own label.

The authors combined images of different channels in order to increase the information content of texture objects.

III. EXPERIMENTAL RESULTS

Artificial and real DI were used for experimental studies. Artificial binary images were generated by a given markup using a mathematical model based on a two-dimensional Markov chain and the algorithm given in [14], [15]. The images were formed in such a way that they contained areas with coincident and different statistical characteristics for different channels.

To assess the accuracy of the selection of the edges of texture objects, the authors compared the segmented image with the ideal markup and then calculated the number of erroneously segmented elements:

$$ESE = \frac{1}{h \cdot w} \sum_{i=1}^h \sum_{j=1}^w F(i, j) \quad (7)$$

where  $h, w$  are image height and width;  $F$  is a value that it equal to zero when the image element is segmented correctly, and equal to 1 if otherwise.

Examples of the results of segmentation of artificial images are shown in Fig. 2: (a) an original image containing two areas with different statistical characteristics ( ${}^1\pi_{ii} = {}^2\pi_{ii} = 0,95$  - for one area and  ${}^1\pi_{ii} = {}^2\pi_{ii} = 0,7$  - for another area); (b) the result of a segmentation algorithm based on an estimate of probability  $\tilde{\pi}_{iii}^{(l,r,k)}$ ; (c) an original image with three objects ( ${}^1\pi_{ii} = {}^2\pi_{ii} = 0,8$  - for the texture area); (d) the result of a segmentation algorithm based on an estimation of probability  $\tilde{\pi}_{iii}^{(l,r,k)}$  and brightness  $\tilde{L}^{(l,r,k)}$ . The image of the  $(k-1)$ -th channel, relative to which segmentation was performed, contained only one texture area with statistical characteristics that coincided with one of the image areas of the  $k$ -th channel.

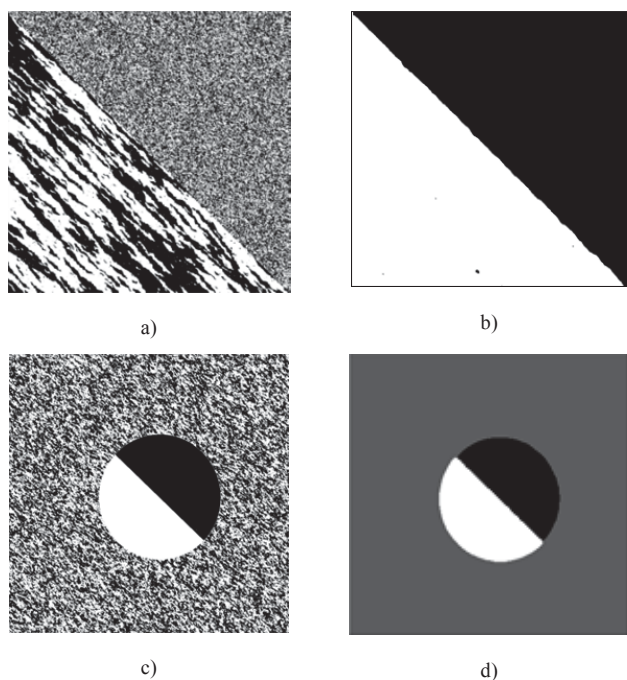


Fig. 2. Results of the segmentation of artificial images

Table II presents the estimates of the ESE criterion for segmented artificial images containing two texture regions (similar to Fig. 2a). A sliding window of 11x11 size was used to calculate the probability estimations  $\tilde{\pi}_{iii}$ .

Three-dimensional segmentation for all values of the transition probabilities gave a segmentation error less than segmentation based on two-dimensional Markov chains. The worst segmentation result was obtained when the difference between the probabilities of the segments was 0.1. As this difference increases, the segmentation error is a fraction of a percent.

TABLE II. EVALUATION OF THE RESULTS OF TWO- AND THREE-DIMENSIONAL SEGMENTATION

Value of transition probabilities ${}^1\pi_{ii}^{(l)} = {}^2\pi_{ii}^{(l)}$		Value ESE, %	
in the first segment	in the second segment	Algorithm based on a two-dimensional Markov chain	Algorithm based on a three-dimensional Markov chain
0,5	0,95	0,32	0,21
0,6	0,9	0,46	0,25
0,7	0,95	0,54	0,28
0,75	0,9	5,45	3,95
0,8	0,9	8,11	5,88

Table III presents the estimates of the ESE criterion for segmented binary images, similar to Fig. 2c. Three-dimensional segmentation was performed on the basis of estimates of probability and brightness characteristics within a sliding window of 11x11.

TABLE III. EVALUATION OF THE RESULTS OF THREE-DIMENSIONAL SEGMENTATION WITH AND WITHOUT BRIGHTNESS

Probabilities between elements in the texture area ${}^1\pi_{ii}^{(l)} = {}^2\pi_{ii}^{(l)}$	ESE,%	
	Without brightness	With brightness
0,6	8,3182	0,61
0,7	8,285	0,5738
0,8	8,1621	0,4429

Accounting for the brightness of the image in a given example allowed to reduce the segmentation error by up to 18 times.

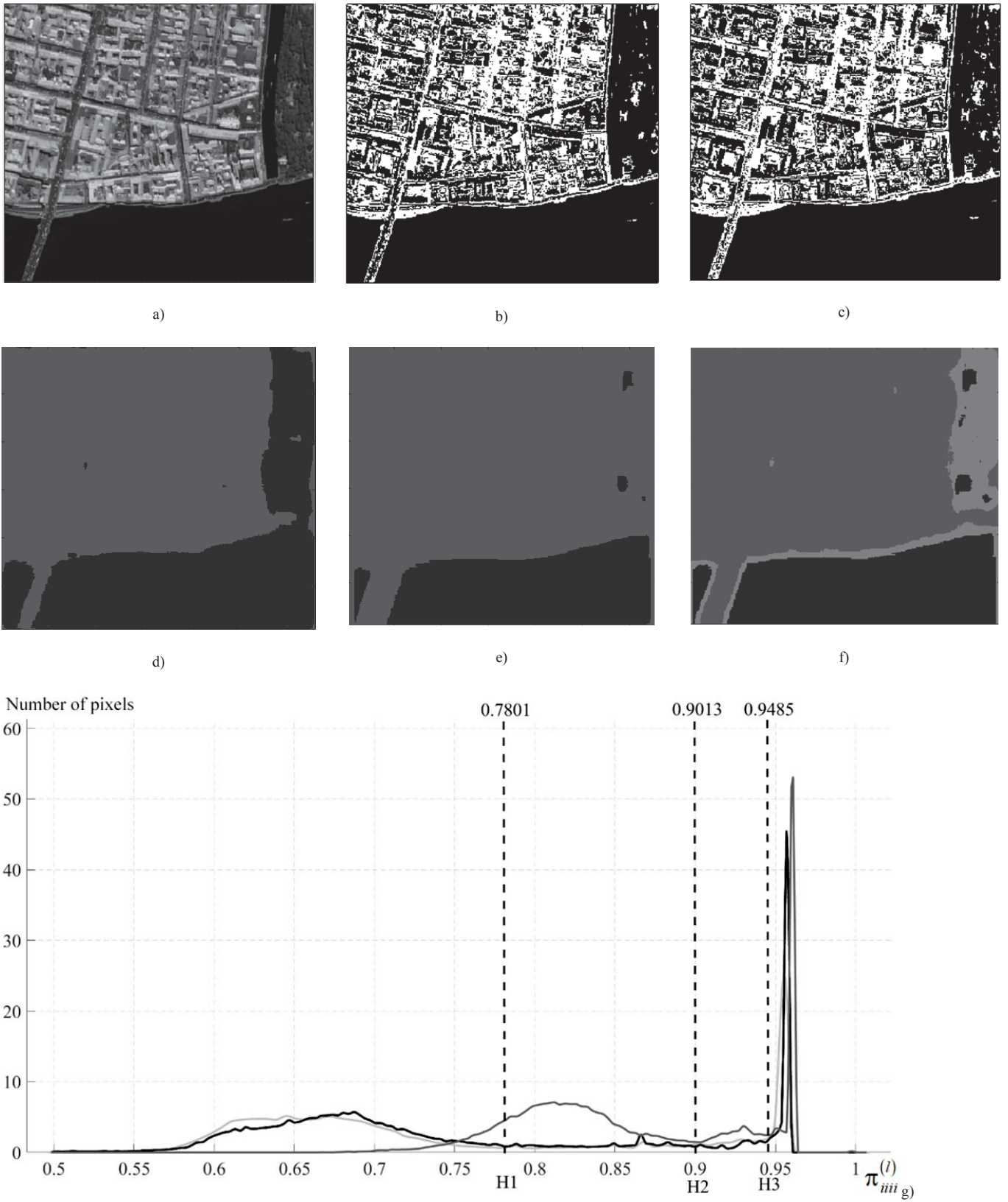


Fig. 3. The result of the detection of texture objects in the remote sensing image

An example of texture-based segmentation on an RGB image, containing three types of objects — urban buildings, park and river — is shown in Fig. 3: (a) — original RGB image; (b) and (c) - BBI of the 7th category of channels R and B, which were used to detect texture objects; (d) and (e) are the results of two-dimensional segmentation of the image of the R and B channels, respectively; (f) - the result of three-dimensional segmentation of channel R relative to channel B; (g) - histograms of a textural feature, on which the selected threshold values are shown with a dotted line (red and blue graphs are obtained from the R and B components, respectively; green - from the component B relative to R). The image size is 400x350 pixels. The size of the sliding window - 11x11 elements.

Two-dimensional segmentation of images of the R and B channels detected only two objects. Three-dimensional segmentation of the image of channel B relative to R made it possible to detect all three objects of an interest. The ratio of correctly segmented pixels is 92.6%.

Thus, combining different channels allow to get information about objects that can not be determined by one channel image.

#### IV. CONCLUSION

The developed segmentation method, based on an estimate of transition probabilities for three-dimensional Markov chains and luminosity, improved the accuracy of detecting the edges of extended texture objects on multichannel compared to the two-dimensional segmentation algorithm proposed in [16]. With statistical characteristics different from 0.45 to 0.1 for different texture regions, the segmentation error is from 0.2 to 6%.

Evaluation of textural features by binary images of the most senior, most informative, digits of a digital image allows to reduce computing resources for the implementation of the segmentation algorithm. Also, the algorithm of three-dimensional segmentation can be applied to detect altered areas on multi-temporal satellite images (deforestation, flooding, burnt areas, etc.).

To increase the stability of the proposed algorithm for detecting texture regions in the presence of noise, a combined method similar to [17], [18], and including a three-dimensional nonlinear filtering algorithm [20], [21] can be used.

#### REFERENCES

- [1] R. A. Schovengerdt, *Remote sensing. Models and methods of image processing*. M.: Technosphere, 2010.
- [2] E.S. Ivanov, "Some applications of remote sensing image segmentation", *Modern problems of remote sensing of the Earth from space*, vol. 13, No. 1., 2016, pp. 105–116.
- [3] R. Gonzalez and R. Woods, *Digital Image Processing*. M.: Technosphere, 2012.

- [4] R.M. Haralick, "Statistical and structural approaches to texture", in *Proceedings of the IEEE*, vol. 67(5), 1979, pp. 786-804.
- [5] M. Li, S. Zang, B. Zhang, S. Li and C. Wu, "A Review of Remote Sensing Image Classification Techniques: the Role of Spatio-contextual Information", *European Journal of Remote Sensing*, vol.47, 2014, pp. 389-411.
- [6] F. Borne, "Texture-based classification for characterizing regions on remote sensing images", *Journal of Applied Remote Sensing*, vol. 11 (3), 2017.
- [7] W. Su, C. Zhang, J. Yang, H. Wu, L. Deng, W. Ou, A. Yue, M. Chen, "Analysis of wavelet packet and statistical textures for object-oriented classification of forest-agriculture ecotones using SPOT 5 imagery", *International Journal of Remote Sensing*, vol. 33 (11), 2012, pp. 3557–3579.
- [8] J. Yuan, D.L. Wang, "Remote sensing image segmentation by combining spectral and texture features", in *IEEE Transactions on geoscience and remote sensing*, vol. 52 (1), 2014, pp. 16-24.
- [9] Z. Kato and J. Zerubia, "Markov Random Fields in Image Segmentation", *Foundations and Trends in Signal Processing*, vol. 5, nos. 1-2 (2011), pp. 1-155.
- [10] Y. Han, H. Kim, J. Choi, Y. Kim, "A shape-size index extraction for classification of high resolution multispectral satellite images", *International Journal of Remote Sensing*, vol. 33, no. 6, 2012. pp. 1682–1700.
- [11] R. Muthukrishnan, M. Radha, "Edge detection techniques for image segmentation", *International Journal of Computer Science & Information Technology (IJCSIT)*, vol. 3, no. 6, 2011, pp. 259–267.
- [12] G. Fu, H. Zhao, C. Li, L. Shi, "Segmentation for High-Resolution Optical Remote Sensing Imagery Using Improved Quadtree and Region Adjacency Graph Technique", *Remote Sensing*, no. 5, 2013, pp. 3259–3279.
- [13] Z. Li. Stan, *Markov Random Field Modeling in Image Analysis*. Springer-Verlag London Limited, 2009.
- [14] E.P. Petrov, I.S. Trubin, E.V. Medvedeva and S.M. Smolskiy, "Mathematical Models of Video-Sequences of Digital Half-Tone Images", *Integrated models for information communication systems and net-works : design and development*. IGI Global, 2013, pp. 207-241.
- [15] E.P. Petrov, E.V. Medvedeva and A.P. Metelyov "Method of synthesis of video images mathematical models based on multidimensional Markov chains", *Nonlinear World*, no. 4, 2011, pp. 213-231.
- [16] E.V. Medvedeva and E.E. Kurbatova, "Image Segmentation Based on Two-Dimensional Markov Chains" *Computer Vision in Control Systems-2. Innovations in Practice*. Springer International Publishing Switzerland, 2015, pp. 277-295.
- [17] E.V. Medvedeva and E.E. Kurbatova, "A combined algorithm of isolation texture areas in noisy images" in *2017 6th Mediterranean Conference on Embedded Computing*, 2017, pp. 155-158.
- [18] E.V. Medvedeva, E.E. Kurbatov and A.A. Okulova, "Textural segmentation of noisy images of the Earth's surface", *Modern problems of remote sensing of the Earth from space*, vol. 14, no. 7, 2017, pp. 20–28.
- [19] L. G. Shapiro and G. C. Stockman, "Computer vision", Prentice Hall, 2001.
- [20] E.V. Medvedeva and I. S. Trubin, "Improving the Noise Immunity of Receiving Video Distorted White Gaussian Noise", in *2016 International Siberian Conference on Control and Communications*, 2016, pp. 7491737.
- [21] E.P. Petrov, I.S. Trubin, E.V. Medvedeva and S.M. Smolskiy, "Development of Nonlinear Filtering Algorithms of Digital Half-Tone Images" in *Integrated models for information communication systems and net-works : design and development*, Aderemi A. Atayero and Oleg I. Sheluhin, editors, PA: IGI Global, 2013, pp. 278-304.